J. Membrane Biol. 104, 147–163 (1988)

The Journal of
Membrane Biology

Deliberate Quin2 Overload as a Method for *In Situ* Characterization of Active Calcium Extrusion Systems and Cytoplasmic Calcium Binding: Application to the Human Platelet

Jonas S. Johansson and Duncan H. Haynes
Department of Pharmacology, University of Miami School of Medicine, Miami, Florida 33101

Summary. The objectives of the title were accomplished by a four-step experimental procedure followed by a simple graphical and mathematical analysis. Platelets are (i) overloaded with the indicator quin2 to cytoplasmic concentrations of 2.9 mM and (ii) are exposed to 2 mM external Ca^{2+} and 1.0 μM ionomycin to rapidly achieve cytoplasmic Ca^{2+} ($[Ca^{2+}]_{cyt}$) of ca. 1.5 μM. (iii) The external Ca^{2+} is removed by EGTA addition, and (iv) the active Ca^{2+} extrusion process is then monitored as a function of time. Control experiments show that the ionophore shunts dense tubular uptake and does not contribute to the Ca^{2+} efflux process during phases iii–iv and that the extrusion process is sensitive to metabolic inhibitors.

The progress curves for the decline of quin2 fluorescence (resulting from active Ca^{2+} extrusion) were analyzed as a function of $[Ca^{2+}]_{cyt}$ using a mathematical model involving the probability that an exported Ca^{2+} was removed from a quin2 complex (*vs.* a cytoplasmic binding element). The observed rates of decline of quin2 fluorescence at a particular $[Ca^{2+}]_{cyt}$ are dependent upon (i) the absolute rate of the extrusion system (a function of its K_m, V_m and Hill coefficient (n)), (ii) the intrinsic Ca^{2+} buffer capacity of the cytoplasm (a function of the total site concentration ($[B]_T$) and its K_d) and (iii) the buffer capacity of the intracytoplasmic quin2 (a function of its concentration and K_d). The contribution of (iii) was known and varied and was used to determine (ii) and (i) as a function of $[Ca^{2+}]_{cyt}$.

The Ca^{2+} binding data were verified by $^{45}Ca^{2+}$ experimentation. The data fit a single binding site ($[B]_T = 730 \pm 200$ μM) with an average K_d of 140 ± 10 nM. This can be accounted for by platelet-associated calmodulin. The rate of the Ca^{2+} extrusion *vs.* $[Ca^{2+}]_{cyt}$ curve can be described by two components: A saturable one with $V_m = 2.3 \pm 0.3$ nmol min^{-1} mg-membrane^{-1}, $K_m = 80 \pm 10$ and $n = 1.7 \pm 0.3$ (probably identified with a Ca^{2+}-ATPase pump) and a linear one (probably identified with a Na^+/Ca^{2+} exchanger).

Key Words platelets, human · calcium transport · Ca^{2+}-Mg^{2+}-ATPase · fluorescent calcium indicators (quin2 and chlorotetracycline) · calmodulin · sodium/calcium exchange

Introduction

Cytoplasmic calcium plays a central role in most, if not all, platelet activation processes (Feinstein, 1982). Studies using the fluorescent chelate probes quin2[1] (Rink et al., 1982; Rink & Sanchez, 1984; MacIntyre, Bushfield & Shaw, 1985; Sage & Rink, 1985) and fura-2 (Rao, Peller & White, 1985; Pollock & Rink, 1986; Pollock, Rink & Irvine, 1986) have shown that resting platelets maintain their $[Ca^{2+}]_{cyt}$ in the 100 nM range. Since the internal Ca^{2+} storage sites in platelets have a finite capacity, this must ultimately be achieved by limiting influx and actively extruding the ion across the plasma membrane.

The extrusion mechanism is not well characterized at present. The plasma membranes of a variety of other cell types are equipped with Ca^{2+}-Mg^{2+}-ATPase (Schatzman, 1982; Carafoli, Zurini & Benaim, 1986) and/or Na^+-Ca^{2+}-exchange (Blaustein & Nelson, 1982; Baker, 1986) proteins that are capable of promoting net Ca^{2+} efflux. A cytochemical study demonstrated Ca^{2+}-Mg^{2+}-ATPase activity associated with platelet surface membranes (Cutler, Rodan & Feinstein, 1978). Membrane fractionation studies have proved to be inconclusive, however, since there are reports both for (Menashi, Davis & Crawford, 1982; Enyedi et al., 1986) and against

[1] Abbreviations used in this paper are as follows: CTC, chlortetracycline; $[Ca^{2+}]_o$, extracellular free Ca^{2+} concentration; $[Ca^{2+}]_{cyt}$, cytoplasmic free Ca^{2+} concentration; $[Q]_T$, concentration of quin2 inside the cells; K_Q, dissociation constant of quin2; $[B]_T$, concentration of the intrinsic cytoplasmic Ca^{2+} binding sites; K_B, dissociation constant of the intrinsic cytoplasmic Ca^{2+} binding sites; EGTA, ethyleneglycol -bis-(*b*-aminoethyl ether)N, N′-tetraacetic acid; quin2, 2-[[2-[bis(carboxymethyl)amino]-5-methylphenoxy]methyl] - 6 - methoxy - 8 - [bis(carboxymethyl) amino]quinoline; HEPES, 4-(2-hydroxyethyl)-1-piperazine-ethanesulfonic acid; fura-2, 1-[2-(5-carboxyoxazol-2-*yl*)-6-amino-benzofuran-5-oxy]-2-(2′-amino-5′-methylphenoxy)-ethane-N,N, N′,N′-tetraacetic acid; Triton X-100, registered trademark of the Rohm and Haas Co. (a mixture of polyoxyethylene ethers and other surface active compounds).

(Steiner & Luscher, 1985; Hack, Croset & Crawford, 1986) the presence of plasma membrane Ca^{2+}-Mg^{2+}-ATPase activity. A recent study based on Na^+-dependent $^{45}Ca^{2+}$ uptake into platelet-derived vesicles reported evidence for the existence of Na^+-Ca^{2+}-exchange activity in the platelet plasma membrane (Rengasamy, Soura & Feinberg, 1987).

The spectroscopic characteristics of quin2 require intracellular dye concentrations of approx. 0.5 mM or more (Grynkiewicz, Peonie & Tsien, 1985). This means that the time course, and the amplitude, of the Ca^{2+} transients being studied may be attenuated. To avoid this drawback, our previous work with this indicator (Jy & Haynes, 1984, 1987; Jy et al., 1987; Shanbaky et al., 1987) has concentrated on steady-state $[Ca^{2+}]_{cyt}$ values.

The present communication shows how the Ca^{2+} buffering potential of quin2 can be used to the investigator's advantage. If the cytoplasm is deliberately overloaded with quin2 and its concentration carefully measured, the fluorometric experiment yields an absolute measure of the number of Ca^{2+} ions moved during a release, influx or extrusion event. We have developed a procedure in which variable quin2 concentrations are used to determine the cytoplasmic binding capacity as a function of the $[Ca^{2+}]_{cyt}$. We verify our findings with $^{45}Ca^{2+}$. We also show how it is possible to determine the kinetics (K_m, V_m and power dependence) of the extrusion system in the platelet plasma membrane.

Materials and Methods

Materials

EGTA, HEPES, quin2/AM, quin2, glucose, 2-deoxy-D-glucose, rotenone, oligomycin and N-methyl-D-glucamine were purchased from Sigma Chemical Co., St. Louis, MO. Chlortetracycline was obtained from ICN Pharmaceuticals, Cleveland, OH, ionomycin from Calbiochem, La Jolla, CA, and $CaCl_2$, NaCl, KCl, $NaHCO_3$, NaH_2PO_4 and Triton X-100 were supplied by Mallinckrodt Inc., Paris, KY.

Platelet Isolation

Whole blood was obtained by antecubital venipuncture from normal healthy donors who denied taking nonsteroidal anti-inflammatory medication for at least the preceding ten days. After discarding the first two ml of blood, 36 ml were drawn into a plastic syringe containing 4 ml of acid-citrate-dextrose anticoagulant (ACD, Fenwal).

The anticoagulated whole blood was centrifuged at 150 × *g* for 10 min in an International Clinical Centrifuge (Model CL) to obtain platelet-rich plasma. A modification of the method of Mustard et al. (1972) was used to separate the platelets from the plasma. Platelet-rich plasma treated with 4 mM EGTA was centrifuged at 600 × *g* for 7 min and the supernatant removed by aspiration. The platelets were then resuspended in a nominally Ca^{2+}- and Mg^{2+}-free Tyrode's solution ($[Ca^{2+}]$ = ca. 1 μM) of the following composition (in mM): 138 NaCl/3 KCl/10 glucose/2 $NaHCO_3$/0.4 NaH_2PO_4/2.5 HEPES with the pH adjusted to 7.35.

Because of the low $[Ca^{2+}]_o$ during the isolation procedure, the platelet Ca^{2+} stores, and cytoplasm, will tend to lose Ca^{2+} as they reach a new steady state. The platelets are therefore referred to as being Ca^{2+} depleted at this point.

Fluorometry

All fluorescence measurements were made using a Perkin Elmer (Model MPF-3L) fluorometer. The selection of filters, stirring, suppression of light scattering artifacts, and choice of wavelengths for quin2 measurements has been described previously (Jy & Haynes, 1987). The suspensions were stirred at 600 rpm and control experiments were performed to assure that the same number of platelets were in the measuring beam throughout the experiment. The measured curves were essentially free of light scattering artifacts. Both the quin2 and the CTC experiments were done at a platelet concentration of 1.6×10^7 per ml in the medium described above at T = 37°C. On a routine basis, the platelet concentration was determined turbidimetrically with a Beckman DB-G grating spectrophotometer as an OD_{600nm} = 0.20. This reading was validated occasionally with a Bright-Line hemacytometer (American Optical).

Quin2 Fluorescence as a Measure of the Average Cytoplasmic Free Ca^{2+} Concentration

Washed platelets suspended in the Tyrode's solution (at a concentration of 2.0×10^8 per ml) were loaded with 5, 10 or 20 μM quin2/AM for 45 min in a modification of the methodology used by Rink et al. (1982). The degree of quin2 loading was determined essentially as described earlier (Jy & Haynes, 1987). Briefly, quin2-loaded platelets were treated with 30 μg/ml digitonin in the presence of 2 mM $[Ca^{2+}]_o$, and the resulting fluorescence signal (F_{max}) was translated into a total quin2 concentration by comparison with a standard quin2 concentration *vs.* fluorescence curve. The corresponding fluorescence in the Ca^{2+}-free state was determined in the presence of 10 mM EGTA. For the present study, the intracellular quin2 concentration was then determined by dividing the total quin2 concentration by the product of the platelet concentration and the platelet volume (taken as 10 fl).

The $[Ca^{2+}]_{cyt}$ was determined using the procedure given in Tsien, Pozzan and Rink (1982). Additional procedures for calibration (Jy & Haynes, 1987) were also applied.

Table 1 shows that the steady-state resting $[Ca^{2+}]_{cyt}$ was not affected by the degree of quin2 loading (for levels between 0.98 and 2.48 mmol quin2 per liter platelet volume). As will be discussed later, this indicates a lack of toxicity or perturbation with regard to the systems involved in Ca^{2+} homeostasis. Rao et al. (1986) found that platelets loaded with quin2/AM at incubation concentrations of up to 80 μM (4× our highest loading concentration) contained normal levels of serotonin and adenine nucleotides, exhibited normal morphology, and failed to show ultrastructural signs of activation.

Table 1. The resting $[Ca^{2+}]_{cyt}$ in platelets loaded with various concentrations of quin2/AM

[Quin2/AM] (μM)	$[Q]_T$[a] (mM)	$[Ca^{2+}]_{cyt}$ (nM)
5	0.98 ± 0.03	104 ± 3
10	1.91 ± 0.07	90 ± 13
20	2.48 ± 0.11	88 ± 9

[a] Calculated as mmol quin2 per liter of cell volume.
The values for $[Ca^{2+}]_{cyt}$ and $[Quin2]_{cyt}$ are given as the mean ± SD with $n = 4$.

Use of CTC Fluorescence as a Measure of Dense Tubular Ca^{2+} Uptake

The techniques used and the proposed mechanism whereby CTC provides a linear measure of the Ca^{2+} accumulation by the dense tubules of human platelets have been detailed in a previous publication (Jy & Haynes, 1987). The probe was used at a standard concentration of 10 μM. The checks against possible artifacts described in that publication were also carried out in the present study. These include lack of contribution by mitochondria or intracellular Mg^{2+} (Jy & Haynes, 1984) and verification that the CTC signal was proportional to both the CTC and to the platelet concentration within the working range. The evaluation of pH artifacts and the contributions of Ca^{2+} in storage granules and membrane exposure accompanying exocytotic release have been made and shown to be negligible (Jy & Haynes, 1984). The manipulation of external Ca^{2+} concentrations (*cf.* Fig. 5) to identify the portion of the CTC signal which is due to dense tubular Ca^{2+} uptake has been described (Jy & Haynes, 1984, 1987) and has proven useful for assessing Ca^{2+} handling derangements in patients with arterial thrombosis and related disorders (Jy et al., 1987; Shanbaky et al., 1987; Ahn et al., 1987). Experiments comparing the two indicators were performed in parallel on the same day. It is not possible to use the two probes simultaneously due to spectral interference (*cf.* Thompson & Scrutton, 1985).

Determination of the K_m of Ionomycin for Ca^{2+}

Washed platelets were loaded at [quin2/AM] = 20 μM and were washed and prepared for fluorometry, as described above. To each sample was added 100 nM ionomycin and varying concentrations of $CaCl_2$ (0.02–100 mM). Solubility constraints set an upper limit on the amount of $CaCl_2$ that could be used. The concentrations of dye and ionophore were selected in order to give the experiment good time resolution. The rate of increase in $[Ca^{2+}]_{cyt}$ from the normal resting level of 100 nM to a value of 200 nM was measured. Constant rates were observed in this interval. For all but the lowest ionomycin concentrations, $[Ca^{2+}]_{cyt}$ rises to higher than 400 within a short time (*cf.* Fig. 1).

$^{45}Ca^{2+}$ Influx into Ca^{2+}-Depleted Cells

Washed platelets, isolated as described above, were suspended at a concentration of 6×10^7 per ml in a plastic cuvette set in a thermostatically-controlled cell holder at 37°C. Influx experiments were started by adding 200 μM Ca^{2+}, together with 4 μCi/ml of $^{45}CaCl_2$ (ICN Radiochemicals, Irvine, CA), to a suspension of the Ca^{2+}-depleted platelets. Aliquots of 300 μl were removed at fixed time intervals, filtered through 0.4-μm Nucleopore filters (Nucleopore, Pleasanton, CA), and washed with Tyrode's solution containing 200 μM Ca^{2+}. Counting was performed with a Tracor Analytic (Model 6892) liquid scintillation spectrometer.

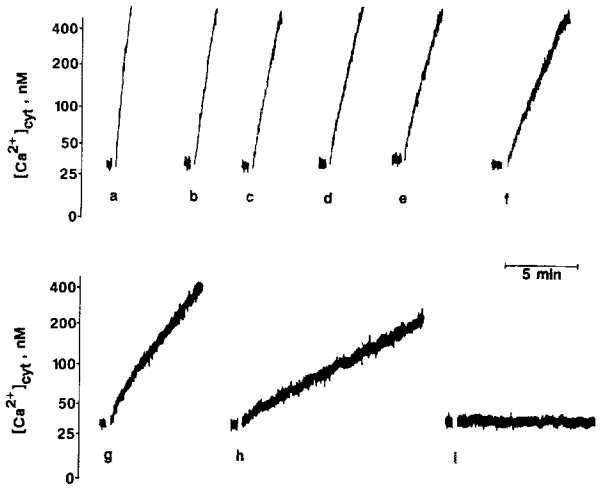

Fig. 1. Examples of progress curves for ionomycin-mediated Ca^{2+} influx into platelets loaded with 3.3 mmol quin2/liter cell volume, at several $[Ca^{2+}]_o$ values. Calibration scales are shown to the left. The discontinuity in each trace indicates the point at which 100 nM ionomycin and the following concentrations of $CaCl_2$ were added: (*a*) 100 mM, (*b*) 50 mM, (*c*) 20 mM, (*d*) 10 mM, (*e*) 5 mM, (*f*) 2 mM, (*g*) 1 mM, (*h*) 0.2 mM, and (*i*) 1 μM

Curve Fitting and Statistics

Best-fit curves and statistics were generated using ASYSTANT (Macmillan Software Company).

Results

Determination of the K_m and Absolute Rate of Ionomycin Movement of Ca^{2+}

Our experimentation uses ionomycin in the presence of external Ca^{2+} as a tool to produce a rapid Ca^{2+} influx into the cytoplasm and to shunt the dense tubular pump system. Ionomycin addition is followed by equally rapid removal of Ca^{2+} from the external medium to allow unopposed efflux through the active extrusion system. This requires the determination of optimal ionomycin concentrations and a knowledge of its kinetics. These were determined *in situ* using the indicator dyes and platelet samples to be studied. Figure 1 shows tracings of the rate of $[Ca^{2+}]_{cyt}$ rise, as monitored with quin2 following addition of 100 nM ionomycin and the indicated con-

Table 2. Values of best fit constants

Constant		Value
$[B]_T$	Total binding sites	0.73 ± 0.20 mM (4.3 ± 1.2 μmol mg^{-1})[a]
K_B	Binding sites	140 ± 10 nM
V_m	Extrusion mechanism	98 ± 8 μM min^{-1}, (2.3 ± 0.2 nmol mg^{-1} min^{-1})[b]
K_m	Extrusion mechanism	80 ± 10 nM
n	Hill Coefficient, above	1.7 ± 0.3
k_{linear}	(Extrusion mechanism, linear component)	16 ± 5 min^{-1}[c] (3.9 ± 1.2 × 10^{-4} liter mg^{-1} min^{-1})[b]
K_m	Ionomycin-catalyzed	7.7 ± 1.0 mM
V_m	Ca^{2+} influx	4.4 mM min^{-1} (Observed for 0.1 μM ionomycin)

The term mM refers to mmol per liter platelet volume.
[a] Given as a concentration per mg total platelet protein.
[b] Given as a rate per mg membrane protein.
[c] Corrected for small ionomycin contribution at $[Ca^{2+}]_{cyt}$ = 1.5 μM.

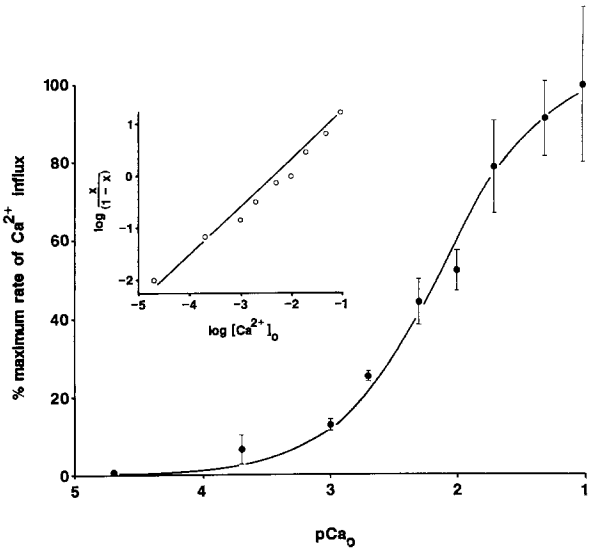

Fig. 2. The normalized rate of ionomycin-catalyzed Ca^{2+} influx into quin2-loaded platelets as a function of $[Ca^{2+}]_o$. Each point represents the mean, and the error bars the SD, of three experiments on the same platelet sample. The solid line is for y values plotted as $y/y_{max} = (106\ [Ca^{2+}]_o)/(K_m + [Ca^{2+}]_o)$, with K_m = 7.74 mM. The inset shows a Hill plot of the same data, with $x = y/y_{max}$

centrations of $CaCl_2$ to Ca^{2+}-depleted platelets (preincubated at $[Ca^{2+}]_o$ = 1 μM). The rates of net Ca^{2+} influx were determined as dFL/dt (linear scale) for 100 nm < Ca^{2+} < 200 for platelets loaded with 3.3 mmol quin2 per liter cell volume (3.3 mM). A rate *vs.* pCa curve and a Hill plot are shown in Fig. 2. The K_m of ionomycin for Ca^{2+} under these conditions, is 7.7 mM, which is in close agreement with the equilibrium constant of 10 mM reported by others (*cf.* Fig. 3 of Bennett, Crockcroft & Gomperts (1979) using the two phase extraction procedure developed by Pressman (1973)). Considering possible experimental errors, the measured Hill coefficient (0.86) is indistinguishable from 1.0. This is in keeping with 1:1 complexation between the ionophore and Ca^{2+} in agreement with Liu and Hermann (1978) and in agreement with the following rate equation:

$$V = (V_m \cdot [Ca^{2+}])/(7.7\ mM + [Ca^{2+}]). \quad (1)$$

In Fig. 1, Trace *a*, 100 nM ionomycin requires ca. 10 sec to increase $[Ca^{2+}]_{cyt}$ from 100 to 200 nM with100 mM $[Ca^{2+}]_o$. With our knowledge of the volume per platelet (10 fl), the platelet concentration, and the total quantity of quin2 trapped (determined from $F_{max} - F_{min}$), we know the average intracellular quin2 concentration ($[Q]_T$ = 3.3 mmol per liter cell volume). It will be shown later in this paper that most of the influxed Ca^{2+} is bound to quin2 at this $[Ca^{2+}]_{cyt}$ and degree of quin2 loading. Using the above, we calculate a V_m of 4.4 mM/min for Ca^{2+} transported into the cell by 100 nM ionomycin. This result and the K_m value are entered into Table 2 and will be used later in this communication.

Monitoring the Active Extrusion of Ca^{2+} from the Cytoplasm with Quin2

Figure 3 shows the basic protocol for studying the active extrusion of Ca^{2+} from the cytoplasm of quin2-loaded platelets. The figure shows the changes in quin2 fluorescence upon the sequential

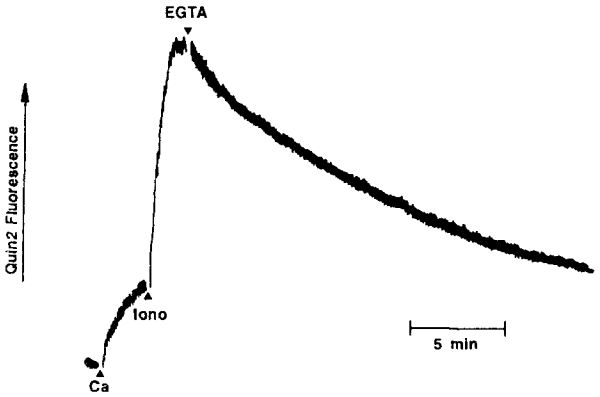

Fig. 3. Changes in quin2 fluorescence induced by the sequential additions of 2 mM $[Ca^{2+}]_o$, 1 μM ionomycin, and 2.7 mM EGTA. The experiment was repeated with 0.1 and 1.0 mM Mg^{2+} and the progress curves were superimposable (*data not shown*)

addition of Ca^{2+}, ionomycin and EGTA. The addition of 2 mM Ca^{2+} causes a gradual rise in the $[Ca^{2+}]_{cyt}$ to ca. 100 nM. This phase represents passive influx opposed by active extrusion and some sequestration. It serves as a control for normal platelet Ca^{2+} handling (*cf.* Jy et al., 1987). Adding 1 μM ionophore results in a rapid increase in the $[Ca^{2+}]_{cyt}$ until probe saturation occurs (allowing for the determination of F_{max}). Using $[Ca^{2+}]_o$ = 2 mM and the data of the previous subsection, the ionophore was operating in the influx mode at 2/7.7th of its K_m and 21% of its V_m. Sufficient EGTA (2.7 mM, using the binding constant data given in Haynes & Mandveno, 1983) is then added to decrease $[Ca^{2+}]_o$ to ca. 100 nM, and the removal of Ca^{2+} from the cytoplasm is followed over time. The fluorescence signal will remain maximal if EGTA is not added, indicating that the observed decrease is not caused by the loss of platelets from the bulk phase or other artifacts. Additional calculations and control experiments (described in another subsection) were done to show that during the EGTA phase the ionophore was operating in the efflux mode at only 1/15400–1/510th of its V_m, and that it did not make a significant contribution to the extrusion process.

Progress curves obtained with 0.1 or 1.0 mM extracellular Mg^{2+} were superimposable on the curve shown in Fig. 3 (nominally Mg^{2+}-free medium). This indicates that either the ionophore is not able to appreciably lower the cytoplasmic free Mg^{2+} concentration during the time course of our experiments or that loss of the same does not affect the pump kinetics. Control experiments also show that the ambient $[Mg^{2+}]_{cyt}$ is expected to make a negligible contribution to the observed fluorescence: When 2 mM Mg^{2+} is added to Ca^{2+}-depleted platelets in the presence of 0.1 μM ionomycin only a small (approx. 2% of $F_{max} - F_{min}$) increase in quin2 fluorescence is observed. Also, calibration experiments with quin2-free acid in Tyrode's buffer and 0.2 mM EGTA showed that addition of 2 mM Mg^{2+} gave a fluorescence increase which was only 2% of the $F_{max} - F_{min}$ observed with saturating Ca^{2+}.

Inhibition of Active Extrusion by Metabolic Inhibitors

Additional experimentation was done to prove that the decrease in quin2 fluorescence during the EGTA phase was the result of a true active extrusion process (*vs.* passive leakage via ionomycin or intrinsic pathways). Figure 4 shows an experiment designed to stop pump activity by depletion of metabolic energy. Platelets were resuspended in a glucose-free medium containing 4 μg/ml oligomycin, 4 μM rotenone and 10 mM 2-deoxy-D-glucose. The sample was preincubated for 16 min. The figure shows the repetition of the normal protocol. After addition of 2 mM Ca^{2+} a slowly developing increase in quin2 signal is observed. The increase was allowed to progress to near saturating levels and then ionomycin and EGTA were added in the normal sequence of Fig. 3. The figure shows that in the EGTA phase the calcium-quin2 signal is maintained at near saturating levels for ca. 40 min. This can be compared to Fig. 3 (no inhibitors) in which the active extrusion process has removed substantial Ca^{2+} from quin2 during the same period. Figure 4 also shows a small instantaneous decrease after the EGTA addition, indicating that a small fraction (7%) of the quin2 was lost from the platelet. This was verified by Mn^{2+} quenching experiments (*not shown*).[2]

Exclusion of Dense Tubular Ca^{2+} Uptake by Efflux Protocol

Figure 5 shows the results obtained when the active extrusion protocol of Fig. 3 was repeated using CTC fluorescence in parallel experiments with the same preparation. The slow phases of fluorescence

[2] The reader wishing to reproduce the experiment of Fig. 4 is cautioned that the optimal time and conditions for metabolic inhibition will vary from one sample to another. Too short an incubation period will result in incomplete inhibition of the extrusion process; too long an incubation period will result in formation of macroscopic aggregates and loss of intracellular quin2, as assessed by Mn^{2+} quenching. It is possible that the platelets within a particular sample have a distribution of sensitivities to metabolic inhibitors.

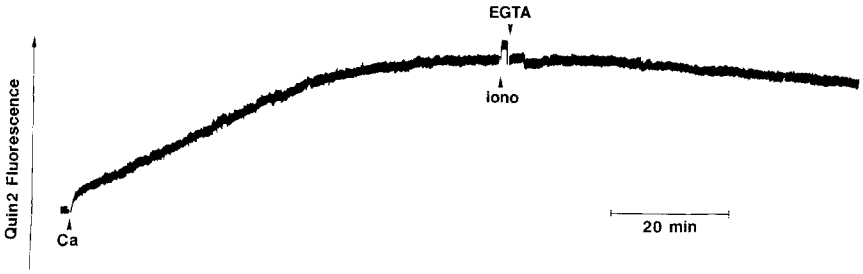

Fig. 4. Inhibition of the active extrusion process by metabolic inhibitors. Experimental conditions are given in the text

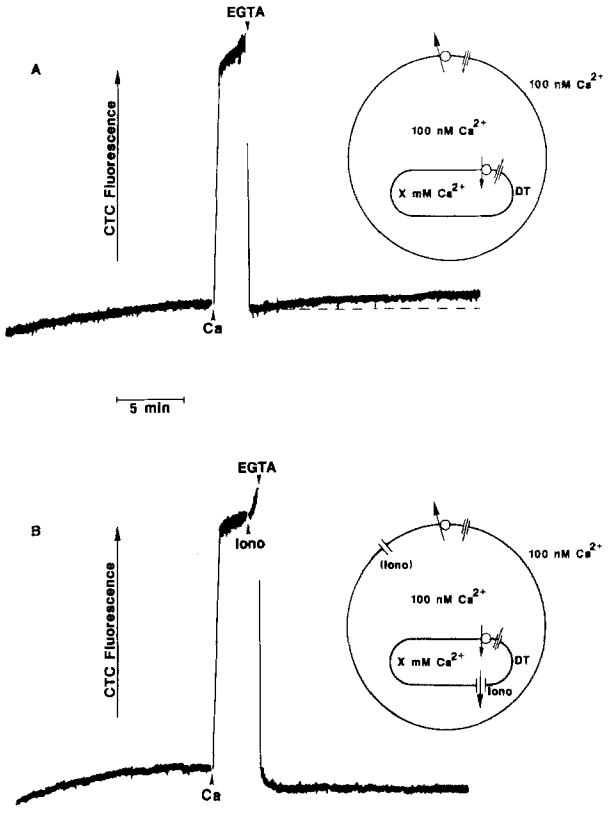

Fig. 5. Abolition of dense tubular uptake with 1 μM ionomycin, reported by CTC fluorescence. Chlorotetracycline (10 μM) was added to Ca^{2+}-depleted platelets (1.6×10^7/ml) at $t = 0$ and then 2 mM Ca^{2+} and 2.7 mM EGTA and 1 μM ionomycin (Panel *B* only) were added where indicated. The right-hand portion of the figure presents schematics giving our interpretation of the experiment. Basal leaks are represented as simple channels; the Ca^{2+} pumps are represented as circles. *DT* and *IONO* denote the dense tubules and ionomycin, respectively

change are due to changes in the level of free Ca^{2+} in the dense tubular lumen (Jy & Haynes, 1984, 1987; Jy et al., 1987). Figure 5*A* shows that Ca^{2+} addition to Ca^{2+}-depleted platelets results in a slow phase of Ca^{2+} uptake into the dense tubules (*cf.* Jy & Haynes, 1984, 1987; Jy et al., 1987). When external Ca^{2+} is removed, this process is attenuated but not immediately abolished, as demonstrated by the much slower increase over baseline in the right-hand portion of the figure. This shows that the dense tubules can compete with the plasmalemmal extrusion system for cytoplasmic Ca^{2+}. Figure 5*B* shows that 1 μM ionomycin increases the rate of dense tubular uptake. As shown previously with A23187 (Jy & Haynes, 1984), this is due to increased uptake through the dense tubular pump, due to the increased $[Ca^{2+}]_{cyt}$. More importantly, the absence of a much slower (post-EGTA) phase in Fig. 5*B* shows that the dense tubules cannot accumulate Ca^{2+} in the presence of 1 μM ionomycin. Thus, the inclusion of the ionophore in our protocol at the chosen concentration has effectively shunted the dense tubular system. This is described schematically in the figure. Effective shunting of the dense tubules is expected because the organelle, by analogy to the skeletal sarcoplasmic reticulum, probably has free internal Ca^{2+} concentrations in the millimolar range (*cf.* Hasselbach & Oetliker, 1983; Haynes & Mandveno, 1987) and the ionophore would be expected to operate on these at rates comparable to those observed in Fig. 1 and described by Eq. (1).

Lack of Ionomycin Contribution to Measured Efflux Rates

The reader may question whether the ionomycin may also be contributing to the efflux rates observed with quin2 in Fig. 3. Using Eq. (1) it can be shown to make no contribution: For operation at between $[Ca^{2+}]_{cyt} = 1500$ nM and $[Ca^{2+}]_{cyt} = 50$ nM, its rate would be 1/510th and 1/15400th of its V_m, respectively. The ionophore-mediated influx with 2 mM extracellular Ca^{2+} takes approx. 2 min. This means that if the ionophore represented the only pathway of extrusion it would require between 4 and 106 hr to reduce $[Ca^{2+}]_{cyt}$ to ca. 50 nM. The time required to clear the cytoplasm is ca. 30 min (*cf.* Fig. 7) so a significant contribution from the ionophore is excluded. This statement is true for all but the highest $[Ca^{2+}]_{cyt}$ (1.5 μM) at which the ionophore contributes only 6% of the total rate of

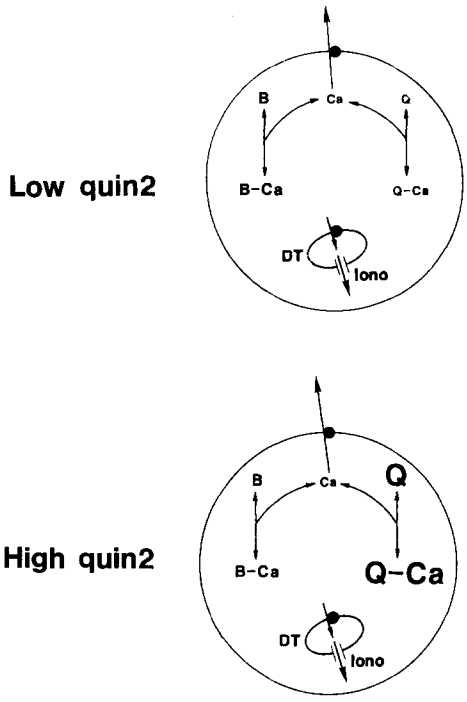

Fig. 6. Schematic representations of platelets loaded with low (or indicator) concentrations of quin2, and high concentrations of quin2. Abbreviations are: *B*, intrinsic cytoplasmic Ca^{2+} binding site; *Ca*, $[Ca^{2+}]_{cyt}$; *Q*, quin2; and *DT*, dense tubular system. The size of the lettering provides a qualitative indication of the concentration of the various components

removal.[3] Also, increasing the ionomycin concentration to 2 μM had no effect on the efflux curve for $[Ca^{2+}]_{cyt} \leq 300$ nM, the region of interest for pump characterization. Also of interest in this regard is the observation that 100 nM ionomycin is not able to make headway against the extrusion system even for $[Ca^{2+}]_o = 1$ μM and $[Ca^{2+}]_{cyt} = 25$ nM. Similar arguments can be applied to intrinsic channels.

In conclusion, this section shows that the Ca^{2+}-plus-ionomycin-followed-by-EGTA maneuver allows us to study the true efflux characteristics of the active extrusion system *in situ*.

The Quin2-Overload Maneuver

Figure 6 shows a schematic of the platelet under two different quin2 loading conditions. The intrinsic cytoplasmic binding sites (*B*) compete with quin2 (Q) for the available free Ca^{2+}. If the cell lacked intrinsic Ca^{2+} binding sites all of the effluxed Ca^{2+} would be taken from the Ca-Q complex and the true efflux would be directly measurable by the indicator. This is, of course, not the case; the Ca^{2+} removed by the extrusion system comes from both Ca-Q and from Ca^{2+} complexes with intrinsic binding sites (Ca-*B*).[4] Our analysis involves the estimation of *P*, the probability that an exported Ca^{2+} was derived from Ca-Q. Two limiting cases can be considered: The "low quin2" and the "high quin2" conditions. The "low quin2" condition, shown in the upper panel, corresponds to the usual situation where the probe is used at low concentration as an indicator of $[Ca^{2+}]_{cyt}$ ($P \ll 1.0$). The rate of Ca^{2+} efflux measured by quin2 fluorescence ($Rate_{obs}$) is much lower than the true rate of Ca^{2+} efflux, which we will define as $Rate_{max}$. The lower panel of Fig. 6 shows the situation where the cell has been deliberately overloaded with the fluorophore. In this case, *P* approaches 1.0 and the quin2 fluorescence becomes a true measure of the numbers of exported Ca^{2+}. The treatment in the Appendix uses the relationship

$$Rate_{obs} = Rate_{max} \cdot P \qquad (2)$$

and shows how the change in *P* with systematic variation of the total quin2 concentration ($[Q]_T$) can be used to determine the total intrinsic cytoplasmic binding site concentration ($[B]_T$). This analysis will be made following a presentation of the experimental data.

Figure 7 shows the quin2 fluorescence versus time curves representing active Ca^{2+} extrusion into a medium of low (100 nM) external Ca^{2+}. Curves *A*, *B*, and *C* are for platelet samples loaded with quin2 concentrations of 2.78, 1.72 and 0.95 mmol per liter cell volume, respectively, determined as described in the Methods. All three curves are plotted on the same absolute fluorescence scale (proportional to [Ca-Q]), with the corresponding $[Ca^{2+}]_{cyt}$ values indicated on their respective scales to the left of the figure. The figure displays the progress curves for the removal of Ca^{2+} from the Ca-Q complex (linear) and for the decrease in the $[Ca^{2+}]_{cyt}$ (nonlinear) for the three degrees of quin2 loading. All curves show initially rapid rates ($-dFL/dt$ or $Rate_{obs}$) which slow for $[Ca^{2+}]_{cyt} < 300$ nM and progress much more slowly for $[Ca^{2+}]_{cyt} < 50$ nM. Lowering of $[Ca^{2+}]_{cyt}$ to less than 20 nM requires approx. 1 hr (*data not shown*).[5]

[3] This calculation is made using Eq. (1) and the V_m and K_m values for ionomycin tabulated in Table 2, taking into account the 10-fold difference in ionomycin values.

[4] The route is dissociation of the complex to give Ca^{2+}_{cyt} which is recognized and exported by the extrusion system.

[5] We also observed that the same time course of fluorescence decrease in the 100 nM > $[Ca^{2+}]_{cyt}$ > 20 nM is observed when the ionomycin step is omitted. If the transient elevation of $[Ca^{2+}]_{cyt}$ did activate the extrusion system (i.e., raise the V_m or lower the K_m), this effect must itself be transient.

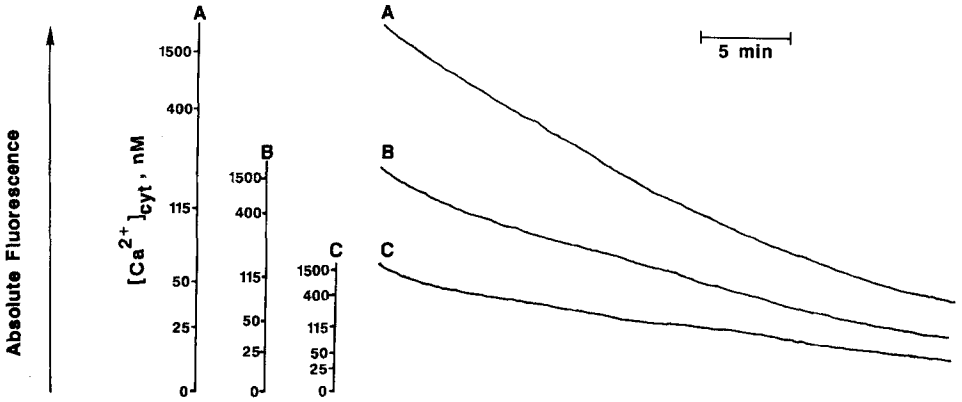

Fig. 7. Progress curves for the removal of Ca^{2+} from the cytoplasm of platelets loaded with three concentrations of quin2. Curve *A* is for 2.78, curve *B* is for 1.72, and curve *C* is for 0.95 mmol quin2 per liter of platelet volume. All curves are drawn on the same absolute fluorescence scale. Calibration scales are shown on the left

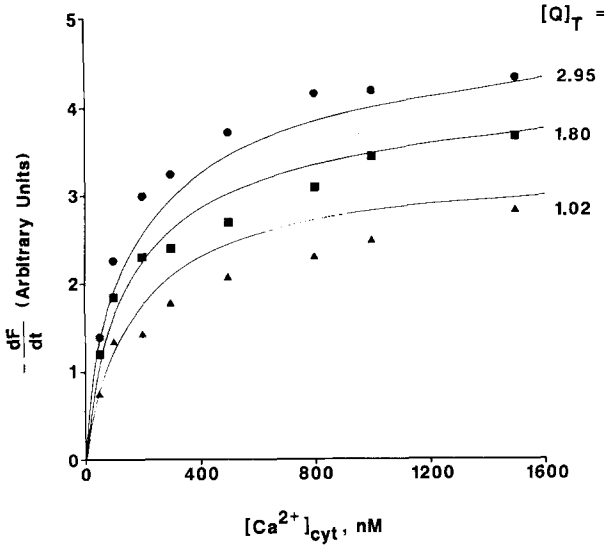

Fig. 8. Absolute rates of changes in fluorescence as a function of the $[Ca^{2+}]_{cyt}$ for the three degrees of quin2 loading shown in Fig. 8. The final quin2 concentrations (in mmol quin2 per liter of cell volume) are given. The continuous lines are theoretical curves, calculated as explained in the last paragraph of the Results

The rates of Ca^{2+} removal from the Ca-Q complex were determined from the slopes of the fluorescence *vs.* time data. The experiment of Fig. (7) was repeated four times with all three degrees of quin2 loading, and the slopes were evaluated for $[Ca^{2+}]_{cyt}$ = 50, 100, 200, 300, 500, 800, 1000, and 1500 nM. The data were normalized and averaged. A smaller number of additional experiments were done to determine the slow rates of efflux for $[Ca^{2+}]_{cyt} < 50$ nM. The dependence of $Rate_{obs}$ on $[Ca^{2+}]_{cyt}$ for the three $[Q]_T$ values is shown in Fig. 8.

Before analyzing these data further it is appropriate to consider the question of whether the high concentrations of cytoplasmic dye could *interfere directly* with the Ca^{2+} handling systems. The resting $[Ca^{2+}]_{cyt}$ at 2 mM external Ca^{2+} would be a reasonable indicator of such interactions since it is determined by the balance between passive leakage across the plasma membrane and the action of the active extrusion mechanism (*cf.* Jy et al., 1987). Table 1 shows the resting $[Ca^{2+}]_{cyt}$ in cells from the same donor sample loaded with 5, 10 and 20 μM quin2/AM (corresponding to 0.98 ± 0.03, 1.91 ± 0.07, and 2.48 ± 0.11, mmol quin2 per liter of platelet volume, respectively). The table shows that all three loading conditions gave essentially the same resting $[Ca^{2+}]_{cyt}$. The values are comparable to those obtained with "indicator" levels of quin2 reported in the literature (Rink & Sanchez, 1984; Sage & Rink, 1985; Jy & Haynes, 1987). This tends to rule out adverse effects, such as Ca^{2+}-Mg^{2+}-ATPase inhibition, attributable to high fluorophore loading.

Determination of the Total Concentration and Average Affinity of the Intrinsic Cytoplasmic Ca^{2+} Binding Sites

The data of Fig. 8 do not show the true kinetics of the extrusion system although the upper curve of that figure gives a good approximation of it. The $Rate_{obs}$ is a function of $Rate_{max}$ and of P which is itself a function of $[Q]_T$ *vs.* $[B]_T$, their respective K_d values and of $[Ca^{2+}]_{cyt}$. The Appendix shows how these factors can be evaluated simply, with no special assumptions other than those of the basic physical chemistry of multiple equilibria. The derivation proceeds from the well-established Ca^{2+} binding relationship for quin2 given by:

$$[Ca\text{-}Q] = ([Q]_T \cdot [Ca^{2+}]_{cyt})/(K_Q + [Ca^{2+}]_{cyt}). \quad (3)$$

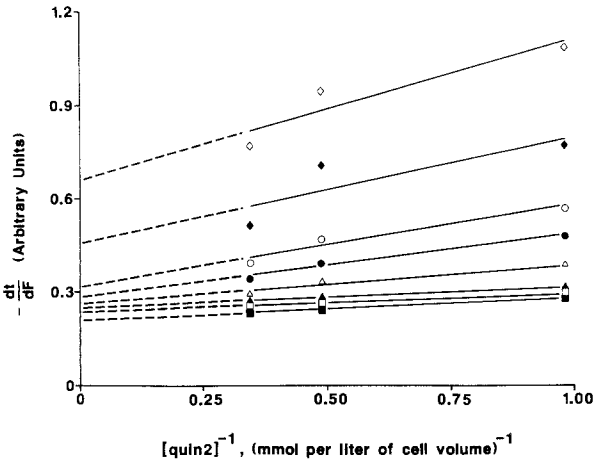

Fig. 9. Plots of $-dt/dF$ *vs.* $1/[Q]_T$ at constant $[Ca^{2+}]_{cyt}$. Data points were fit by linear regression to give the solid lines. Points represent the mean of six experiments on three different platelet samples. Error bars are omitted for clarity. Calculated standard deviations averaged 11.3% of the mean

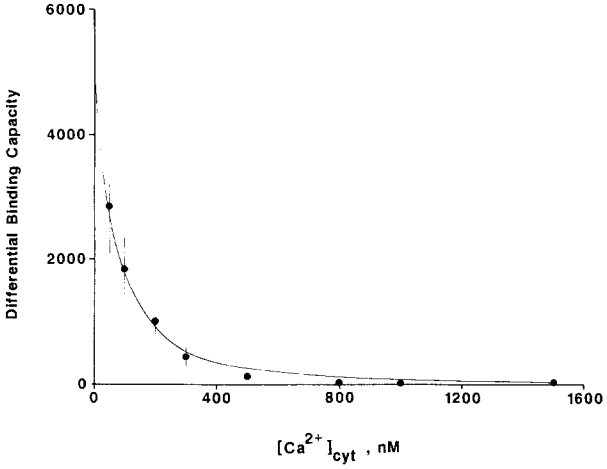

Fig. 10. The differential binding capacity of the intrinsic cytoplasmic Ca^{2+} binding sites as a function of $[Ca^{2+}]_{cyt}$. The solid line is a best fit curve generated using the equation $DBC = ([B]_T \cdot K_B)/(K_B + [Ca^{2+}]_{cyt})^2$, with $[B]_T = 0.730$ mM and $K_B = 140$ nM. The equation is analogous to Eq. (A3). The *y*-intercept is equal to $[B]_T/K_B$ (= 5,210) and the K_B value is equal to the $[Ca^{2+}]_{cyt}$ for which *y* is one-fourth of the *y*-intercept value. The error bars represent standard deviations for the DBF which are determined by the standard deviations of the calculated $[Q]_{T,1/2}$ values from Fig. 9. For the four points at the highest $[Ca^{2+}]_{cyt}$ the standard deviations ranged from 25–50%

We define the first derivative of Eq. (3) with respect to $[Ca^{2+}]_{cyt}$ as its "differential binding capacity" (DBC), with

$$DBC = d[\text{Ca-Q}]/d[Ca^{2+}]_{cyt} = ([Q]_T \cdot K_Q)/(K_Q + [Ca^{2+}]_{cyt})^2. \quad (4)$$

It is possible to write equations corresponding to Eqs. (3) and (4) for each of the intrinsic cytoplasmic binding elements. However, since their number and characteristics are not pre-determined we choose to use their DBC ($d[\text{Ca-}B]/d[Ca^{2+}]_{cyt}$) to define them. The appendix shows that the value of *P* is given by

$$P = \frac{\dfrac{[Q]_T \cdot K_Q}{(K_Q + [Ca^{2+}]_{cyt})^2}}{\dfrac{[Q]_T \cdot K_Q}{(K_Q + [Ca^{2+}]_{cyt})^2} + \dfrac{d[\text{Ca-}B]}{d[Ca^{2+}]_{cyt}}}. \quad (5)$$

The constants relating to quin2 are known quantities. The value of K_Q is taken as 115 nM (Tsien et al., 1982) and $[Q]_T$ and $[Ca^{2+}]_{cyt}$ are known. For any particular $[Ca^{2+}]_{cyt}$, the condition $P = 0.5$ corresponds to half-maximal rate (*vs.* infinite $[Q]_T$) and the DBC of the cytoplasmic elements is readily determinable as

$$\frac{d[\text{Ca-}B]}{d[Ca^{2+}]_{cyt}} = [Q]_{T,1/2} \cdot \frac{K_Q}{(K_Q + [Ca^{2+}]_{cyt})^2} \quad (6)$$

where $[Q]_{T,1/2}$ is the concentration of quin2 (mole per liter cell volume) giving half-maximal rate (at a particular $[Ca^{2+}]_{cyt}$).

The most tractable means of analysis is a double reciprocal plot of the $Rate_{obs}$ *vs.* $[Q]_T$ data. Equation (A11) of the Appendix gives

$$(1/Rate_{obs}) = 1/Rate_{max}\left(1 + \frac{d[\text{Ca-}B]/d[Ca^{2+}]_{cyt}}{[Q]_T \cdot \dfrac{K_Q}{(K_Q + [Ca^{2+}]_{cyt})^2}}\right) \quad (7)$$

which predicts a linear double reciprocal plot, with the true rate of the pump given by the reciprocal of the *y* intercept and the DBC of the cytoplasmic elements defined by the conditions of half-maximal rate and Eq. (5).

Figure 9 is a replot of the data of Fig. 8 according to Eq. (7). Linearity and a positive slope are observed for all of the analyzed $[Ca^{2+}]_{cyt}$ values.[6] Values of $[Q]_{T,1/2}$ were determined and the corresponding $d[\text{Ca-}B]/d[Ca^{2+}]_{cyt}$ values were calculated using Eq. (5). The result is presented in Fig. 10. The continuous line is the best fit of the data according to the derivative equation described in the figure legend. The conformance shows that the cytoplasmic binding elements can be described as a single class of noninteracting sites according to

$$[\text{Ca-}B] = [B]_T \cdot \frac{[Ca^{2+}]_{cyt}}{[Ca^{2+}]_{cyt} + K_B} \quad (8)$$

[6] If the binding site or its contribution had been absent, horizontal lines would have been predicted by Eq. (7).

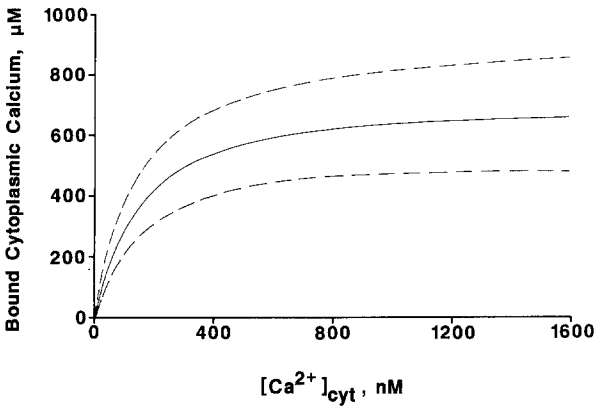

Fig. 11. Theoretical plot showing the occupation of intrinsic cytoplasmic binding sites as a function of $[Ca^{2+}]_{cyt}$. The solid line has the form Ca-B = (730 μM · $[Ca^{2+}]_{cyt}$)/(140 nM + $[Ca^{2+}]_{cyt}$). The dashed lines are fits of the envelope defined by the standard deviations in Fig. 10. The upper and lower lines correspond to $[B]_T$ and K_B values of 930 μM and 140 nM, and 530 μM and 140 nM, respectively

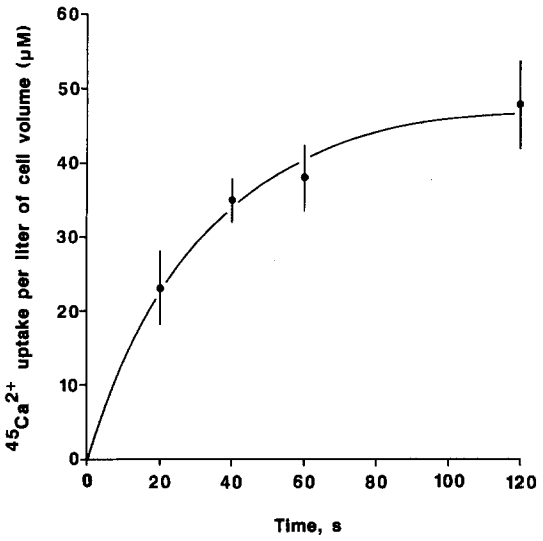

Fig. 12. Kinetics of net $^{45}Ca^{2+}$ influx into Ca-depleted platelets. Points and error bars represent the mean ± SD of four different sets of experiments consisting of three runs each. The data are fitted with the equation Ca^{2+} influx = 48.2 (1.0 − exp(− 0.0304 × t)), with t given in sec

with $[B]_T$ = 730 ± 200 μM and K_B = 140 ± 10 nM. The calculated binding characteristic is shown in Fig. (11).

$^{45}Ca^{2+}$ Experimentation

To test the validity of the derived constants for the intrinsic cytoplasmic Ca^{2+} binding sites we used $^{45}Ca^{2+}$ influx into Ca^{2+}-depleted platelets, carried out as described under Materials and Methods. The

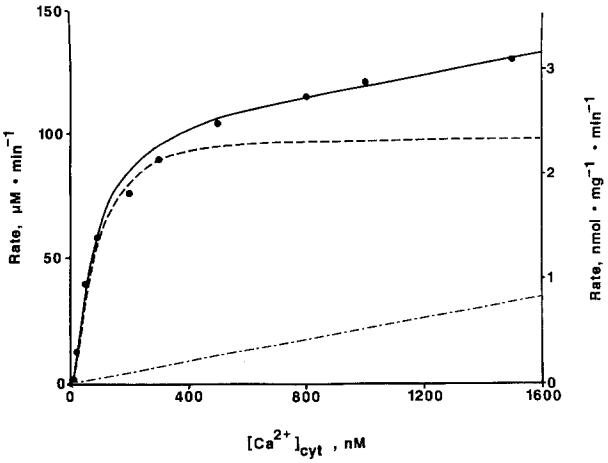

Fig. 13. The calculated true rate of the efflux mechanism as a function of $[Ca^{2+}]_{cyt}$. The solid line has the form $Rate_{max} = ((V_m \cdot [Ca^{2+}]^n_{cyt})/(K^n_m + [Ca^{2+}]^n_{cyt})) + k \cdot [Ca^{2+}]_{cyt}$, with V_m = 98 ± 8 μM min^{-1}, K_m = 80 ± 10 nM, n = 1.7 ± 0.3, and k = 16 ± 5 min^{-1}. Rate units on the left were calculated using the rate data obtained from platelets loaded with the highest degree of quin2 (giving concentrations of 3.07 ± 0.29 mM dye per liter of cell volume) using $Rate_{max} = -dF/dt \cdot 1/(F_{max} - F_{min}) \cdot [Q]_T \cdot 1/P$. The value of ($F_{max}$ − F_{min}) is the difference in the fluorescence signal recorded between full probe saturation with Ca^{2+} and that of the uncomplexed probe. The rate units on the right were calculated from the left-hand scale, using 10 fl/platelet and 170 mg platelet protein = 10^{11} platelets. The experimental data were obtained from Fig. 8 and were supplemented by more extensive data obtained at high $[Q]_T$ and long-term efflux experiments probing the behavior at $[Ca^{2+}]_{cyt}$ < 50 nM

differences between these experiments and the fluorometric ones lie in the selection of platelet and external Ca^{2+} concentrations. It was necessary to use a lower $[Ca^{2+}]_o$ value in the $^{45}Ca^{2+}$ experiment in order to achieve an acceptable signal-to-background ratio. The experiment measured isotopic influx under conditions of net movement. Figure 12 shows that 48.2 μM Ca^{2+} is taken up per liter of cell volume. In the Discussion section we show that this is in excellent agreement with the predictions of quin2 experiments for $[Ca^{2+}]_o$ = 0.2 mM. The half-time of 22.6 sec is in fair agreement with that measured for reaching the new steady state in the fluorometric experiments after the addition of 2 mM Ca^{2+} to platelets loaded with "indicator" concentrations of quin2 (48 ± 8 sec, n = 4, for 0.98 ± 0.03 mmol quin2 per liter of cell volume, *data not shown*).

Determination of the True Rate of the Plasma Membrane Ca^{2+} Extrusion System

Having determined the characteristics of the intrinsic Ca^{2+} binding sites, we can use Eq. (2) to calculate the true rate of the extrusion system based on the observed rate obtained with platelets loaded with our highest degree of quin2. Figure 13 presents

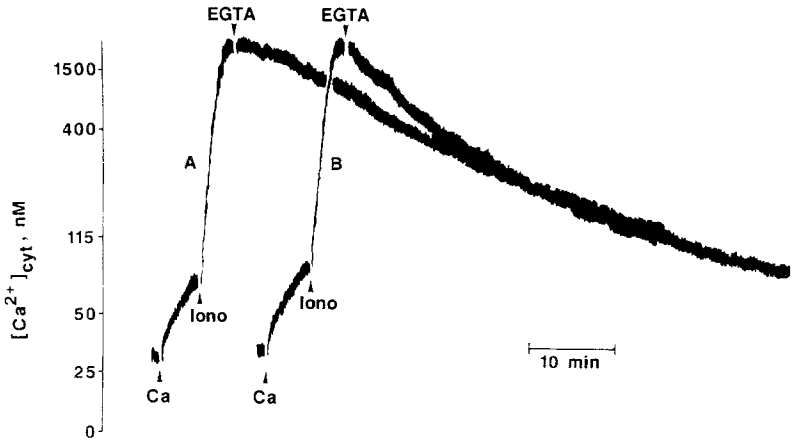

Fig. 14. Effect of N-methylglucamine for Na^+ substitution on the progress curve for active extrusion. Experiments were done according to the normal protocol with the following exceptions: In curve *A*, cells were resuspended in the normal medium modified to contain 10 mM NaCl and 124 mM N-methyl-D-glucamine chloride. In curve *B*, the cells were suspended in normal medium containing 134 mM NaCl. The quin2 concentration was 3.2 mmol/liter cell volume

the $[Ca^{2+}]_{cyt}$ dependence of $Rate_{max}$. The left-hand scale gives the rate as mmol Ca^{2+} transported per minute per liter platelet volume. The right-hand scale expresses the rate in the more conventional units (nmol mg^{-1} min^{-1}). The constants used in these calculations are 10 fl/platelet and 10^{11} platelets = 170 mg platelet protein (of which 25% is membrane associated; *cf.* Sixma & Lips, 1978).

The data are fitted to the following equation

$$Rate_{max} = (V_m \cdot [Ca^{2+}]^n_{cyt})/(K^n_m + [Ca^{2+}]^n_{cyt}) + k_{linear} \cdot [Ca^{2+}]_{cyt} \quad (9)$$

with V_m = 98 μM/min, K_m = 80 nM, n = 1.7 and k_{linear} = 16 min^{-1}.* These data are tabulated in Table 2. We believe that the first term describes the behavior of the plasmalemmal Ca^{2+}-Mg^{2+}-ATPase pump. Table 2 summarizes the values of the constants calculated in this study.

The second term describes a component which does not saturate for $[Ca^{2+}]_{cyt}$ in the range studied. It may be tentatively identified with a Na^+/Ca^{2+} exchanger. Since some discussants have expressed interest in this point, an additional experiment supporting the interpretation has been included in the present study. Figure 14 compares the active extrusion characteristics in the presence and absence of external Na^+. The figure shows that substitution of N-methylglucamine for Na^+ results in slower initial rates of Ca^{2+} removal, as would be expected for the case where a sizable contribution of a Na^+/Ca^{2+} exchanger is eliminated. At longer times and $[Ca^{2+}]_{cyt} \leq 220$, the extrusion curves are congruent. This is expected for the case where the linear (Na^+/Ca^{2+} exchange) term makes a smaller relative contribution. The control curve has been shifted to the right for ease of comparison.

* The k_{linear} value is corrected for a 25% contribution of the ionomycin to the linear process, calculated from Eq. (1) and the associated data.

Further Validation of Procedure and Model

One frequently-raised objection to mathematical modeling of biological systems is that the latter are inherently complex and that it is always possible to fit any sort of behavior with a small number of constants. The unstated concern is that there may be some critical aspect of the studied system not encompassed by the model or that the final model and derived constants may fail to predict this feature. This concern is addressed in Fig. 8. The continuous curves, which give excellent fits of the experimental data, were generated using Eqs. (6)–(9), the constants of Table 2 and the data of Fig. 10. It can also be shown that the rate and *P* equations of the text, together with the constants of Table 2, can be numerically integrated to give excellent fits of the experimentally-determined efflux curves. This supports our conclusion that our results do represent the true behavior of the extrusion system operating *in situ* and that these results can be discussed as such.

Discussion

Our results show that the quin2 overload method can be used to determine the cytoplasmic buffering characteristics and the true kinetics of the efflux system. This has the advantage that these important properties can be studied *in situ* with minimal perturbation of the cell and the system to be measured. At low or intermediate quin2 concentrations the intrinsic cytoplasmic Ca^{2+} binding sites will distort the true rate of efflux to an extent that depends on the $[Q]_T$ and the $[Ca^{2+}]_{cyt}$. At high quin2 concentrations the observed rate will approach the true rate, reported in convenient linear fashion by quin2 fluorescence.

The quin2 overload method can also be applied to the quantitative measurement of Ca^{2+} move-

ments between intracellular pools, as with release from the dense tubular system. Parallel experiments using CTC fluorescence are a useful adjunct to the method. The quin2 overload method also allows the Ca^{2+} extrusion system to be studied in various metabolic states and states of activation.

Comparison with $^{45}Ca^{2+}$ Study

Our determination of the intrinsic cytoplasmic binding site characteristics using the quin2 method is corroborated by the $^{45}Ca^{2+}$ experiments, and vice versa. Unfortunately, it was not possible to repeat our standard Ca^{2+} challenge experiment with 2 mM external Ca^{2+} (*cf.* Jy et al., 1987) using the $^{45}Ca^{2+}$ and filtration methods because the background counts and zero-time controls were too large. However, good agreement can be shown between the quin2 and the isotope experiments when $[Ca^{2+}]_o$ is jumped to 0.2 mM, a value chosen to obtain acceptable signal-to-noise ratios in the isotope experiment and to achieve conditions comparable to those of Brass (1984*a*,*b*, 1985).

Our quin2 experimentation shows that Ca^{2+}-depleted platelets ($[Ca^{2+}]_o$ = 1 μM) have a resting $[Ca^{2+}]_{cyt}$ = 40 μM. Use of Eq. (8) and the determined $[B]_T$ and K_B values predicts that the total cytoplasmic Ca^{2+} will be equal to 162 μmol/liter cell volume. We have observed that when $[Ca^{2+}]_o$ is jumped to 0.2 mM, $[Ca^{2+}]_{cyt}$ becomes 60 nM. Equation (8) predicts that the total cytoplasmic Ca^{2+} will be equal to 219 μmol/liter cell volume. The difference corresponds to the net influx of 57 μmol/liter Ca^{2+} into the cytoplasmic compartment. This is in fair agreement with our finding of 48.2 μmol/liter $^{45}Ca^{2+}$ influx. Also, the kinetics of the equilibration as reported by quin2 and $^{45}Ca^{2+}$ are comparable (*compare* Fig. 12 with Fig. 3 for quin2-overloaded or Fig. 1 of Jy and Haynes (1987) for quin2-lightly-loaded platelets).

The above results can be compared with cytoplasmic pool sizes of 52–54 μmol/liter measured under steady-state conditions at 0.2 mM $[Ca^{2+}]_o$ (Brass, 1984*a*,*b*, 1985) exchanging with a $t_{1/2}$ of 17 min. The difference in $t_{1/2}$ may be explained by isotopic equilibration requiring more time than net influx. Further interpretation of these results is probably not warranted in the present publication. The process of net influx to give a higher degree of Ca^{2+} saturation of B is fundamentally different from the process of isotopic equilibration in which the degree of Ca^{2+} saturation is constant, but "cold" Ca^{2+}-B must be replaced by $^{45}Ca^{2+}$-B. The former case requires only that the influxed Ca^{2+} bind to B, whereas the latter case requires that $^{45}Ca^{2+}$ enter the cell, bind to B, and that cold Ca^{2+}-B must liberate Ca^{2+} and that the liberated Ca^{2+} be exported by the pump, rather than bind to another B. Also, the contributions of the dense tubules must be considered for equilibration times in the >5 min range. We believe that further experimentation together with stochastic modeling of these processes is justified.

Free vs. Bound Ca^{2+}

Our study underscores an important feature of cytoplasmic Ca^{2+} of the human platelet: That the free ("ionized") Ca^{2+} is only a small fraction of the total cytoplasmic Ca^{2+}. Simple calculations using the data of Table 2 show that the free cytoplasmic Ca^{2+} is only 1/2700th of the total cytoplasmic Ca^{2+} under resting conditions with $[Ca^{2+}]_o$ = 2 mM. Our values for the concentration, and average affinity, of the intrinsic cytoplasmic Ca^{2+} binding sites are comparable to those obtained by von Tscharner, Deranleau and Baggiolini (1986) in neutrophils, using a similar method.

Role of Calmodulin

The present study identified a single class of Ca^{2+} sites in the $[Ca^{2+}]_{cyt}$ range studied (32–1,500 nM, or more conservatively 32–500 nM). Undoubtably other sites would have been revealed by methods capable of measuring binding in the 1.0–100 (+) μM range. The sites quantitated in the present study ($[B]_T$ = 730 ± 200 μM; K_B = 140 ± 10 nM) can be accounted for by calmodulin which is present in appreciable concentrations (*cf.* Feinstein, 1982). White, Levine and Steiner (1981) estimated the concentration to be 26.5 fg per cell (1.6% of total protein), which translates into 0.16 mM, assuming a volume of 10 fl and exclusive location within the cytoplasmic compartment. Since each calmodulin molecule has four Ca^{2+} binding sites, this would represent 0.64 mM (or 88%) of our reported $[B]_T$. Other less abundant Ca^{2+}-binding proteins would also be expected to contribute. The dissociation constants of the four Ca^{2+} binding sites for the molecule in free solution are in the order of 10^{-6} M, but the K_B can be as low as 10^{-8} M when the molecule is bound to another cell component (Kohse & Heilmeyer, 1981). Thus our average K_B of 1.4×10^{-7} M is in the correct range for calmodulin. It is probable that Ca-calmodulin complexes, particularly those with 3:1 and 4:1 stoichiometry, are important transducers of the Ca^{2+} signal in the human platelet. If the binding activity which we have observed does indeed represent the bound form of calmodulin with four noninteracting sites, the fraction of the calmodulin in the higher complexes would be 0.085 or

0.037 at rest ($[Ca^{2+}]_{cyt}$ = 110 nM) and would be 0.41 or 0.30 at the $[Ca^{2+}]_{cyt}$, giving half-maximal rate of aggregation (400 nM, *cf.* Jy & Haynes, 1987). In this regard, it is significant that the aggregation rate has a (saturating) fourth power dependence on $[Ca^{2+}]_{cyt}$ (Jy & Haynes, 1987).

Abundance of the Extrusion Pump

Our kinetic results can also be related to biochemical studies of the platelet membrane. In a review dealing with membrane isolation, Sixma and Lips (1978) calculated that 25.3% of the total platelet protein (given as 170 mg per 10^{11} cells) is present in membranes. Using these values, and taking a value of 10 fl for the volume of a single platelet, allows one to recalculate our results in terms of membrane protein. Thus the V_m of 98 μmol min^{-1} $liter^{-1}$ (platelet volume) becomes 2.3 nmol Ca^{2+} min^{-1} mg^{-1} (membrane protein). Table 2 also presents these constants in the alternative units. Published values for maximal Ca^{2+}-Mg^{2+}-ATPase activity in isolated platelet plasma membranes range from 0.038 (Menashi et al., 1982) to 3.5 (Enyedi et al., 1986) nmol Ca^{2+} mg^{-1} min^{-1}. Our value is in fair agreement with the latter value. Values for K_m and Hill coefficient are not available for the isolated plasma membrane.

It is also possible to estimate the abundance of the pump. If the pump has a turnover number of 10 sec^{-1} (*cf.* Verjovski-Almeda & Inesi, 1979; Chiu & Haynes, 1980, giving values of 5 to 12 sec^{-1} for skeletal sarcoplasmic reticulum Ca^{2+}-Mg^{2+}-ATPase) an abundance of approx. 1,000 pumps per platelet can be calculated. This corresponds to 70 pump molecules per μm^2, using 15 μm^2 as the surface area of a human platelet (Stahl, Themann & Dame, 1978). In terms of mg plasma membrane the pump density corresponds to 0.055% of the membrane protein, assuming 140 kDa as the molecular weight of plasma membrane Ca^{2+}-Mg^{2+}-ATPases (*cf.* Carafoli et al., 1986). As a comparison, Niggli, Penniston and Carafoli (1979) have estimated that the Ca^{2+}-Mg^{2+}-ATPase of the erythrocyte plasma membrane accounts for ca. 0.1% of the total protein present.

Properties of the Extrusion System

Our results are typical of the extrusion system working at 1 mM intracellular Mg^{2+} and ambient intracellular pH. The effects of variation of the latter deserve further study, with respect to both the indicator properties of quin2 and the known pH sensitivity of Ca^{2+} transport ATPases (Haynes & Mandveno, 1987). It should be mentioned that our quin2 measurements give the average free cytoplasmic Ca^{2+} concentration and that this is the same parameter to which the pump responds.

It should also be noted that our protocols cause a transient activation of the platelets as an unavoidable consequence of raising $[Ca^{2+}]_{cyt}$ above 400 nM, the K_m for aggregation. In most of our experiments $[Ca^{2+}]_{cyt}$ rose from 110 nM to 1.5 μM in the 1.5 min of the "ionomycin plus 2 mM Ca^{2+} phase." These conditions were undoubtably sufficient to produce the shape change and exocytotic release reaction but were not adequate to give much formation of higher aggregates. What aggregation had occurred was reversed in the subsequent "EGTA phase." Within approx. 7.5 min after EGTA addition, $[Ca^{2+}]_{cyt}$ returned to 400 nM. Thus the duration of exposure to "activating" $[Ca^{2+}]_{cyt}$ values was approx. 9 min. Although it is conceivable that the above manipulations cause the pump to be activated by an as yet to be identified biochemical mechanism, our findings suggest otherwise. If there were an activation, it must be as short as the Ca^{2+} transient itself (i.e., <22 min) since the extrusion progress curve for $[Ca^{2+}]_{cyt} \leq 100$ nM is identical for samples which have or not had a history of $[Ca^{2+}]_{cyt}$ = 1.5 μM. Thus we believe that we have studied the extrusion system in a stable state.

Figure 13 shows the saturable extrusion system to be responsible for the major portion of efflux over the range for $[Ca^{2+}]_{cyt} < 1.5$ μM. The saturable system has the characteristics of a Ca^{2+}-Mg^{2+}-ATPase pump. The K_m of 80 nM is in line with values for this enzyme in the sarcolemma (0.3 ± 0.2 μM, Caroni & Carafoli, 1981; "about 0.5 μM," Carafoli, 1985) and squid axon (0.18 μM, *cf.* DiPolo & Beauge, 1983). Our Hill coefficient of 1.7 (i.e., $1 < n \leq 2$) is expected for a Ca^{2+}-Mg^{2+}-ATPase pump with a stoichiometry of 2 Ca^{2+} per ATP split. This arrangement is not only optimal from the biophysical (Haynes & Mandveno, 1983) and thermodynamic (Trevorrow & Haynes, 1984) viewpoints, but also from the standpoint of tight regulation of resting $[Ca^{2+}]_{cyt}$. In the long term, the latter is governed by the competition between passive influx through the leak (and channel) mechanisms and the active extrusion

$$d[Ca^{2+}]_{in}/dt = k_{leak}[Ca^{2+}]_o - (V_m \cdot [Ca^{2+}]^n_{cyt})/(K^n_m + [Ca^{2+}]^n_{cyt}) - k_{linear} \cdot [Ca^{2+}]_{cyt} \quad (10)$$

where k_{leak} is the rate constant for passive leakage and where the other terms are as defined in Eq. (9). At steady-state, $[Ca^{2+}]_{cyt}$ becomes time-invariant

and $d[Ca^{2+}]_{in}/dt = 0$. Neglecting the contributions of k_{linear} and rearranging gives

$$[Ca^{2+}]_{cyt} = K_m \left(\frac{k_{leak}[Ca^{2+}]_o}{V_m - k_{leak}[Ca^{2+}]_o}\right)^{1/n}. \quad (11)$$

Substitution of the present values gives

$$[Ca^{2+}]_{cyt} = 80 \text{ nM} \cdot \left(\frac{k_{leak}[Ca^{2+}]_o}{98 \ \mu\text{M/min} - k_{leak}[Ca^{2+}]_o}\right)^{1/1.7}. \quad (12)$$

The actual resting $[Ca^{2+}]_{cyt}$ is close to the K_m. For $[Ca^{2+}]_{cyt} = 110$ nM the pump is operating at 63% of its maximal velocity and Eq. (12) is satisfied by $k_{leak}[Ca^{2+}]_o = 0.63\ V_m = 62\ \mu$M/min.

The 1/1.7 power dependence in Eq. (12) helps somewhat improve on the low safety factor inherent in the denominator of that equation. However, sharp increases in $[Ca^{2+}]_{cyt}$ are nevertheless predicted as $k_{leak}[Ca^{2+}]$ is increased to become comparable to V_m. The contributions of the nonsaturable component (neglected in Eqs. (11) and (12) then become a crucial safety factor to prevent an explosive increase in $[Ca^{2+}]_{cyt}$. It is of interest that we have found that platelets from patients with arterial thrombosis have mean resting $[Ca^{2+}]_{cyt} = 170$ nM. The increase was shown to be due to increased influx through a verapamil-sensitive channel. Application of the above reasoning predicts that the Ca^{2+} pump was working at 78% of its V_m and that the increase over normal was due to opening of sufficient channels to increase the influx rate approx. 23% over basal level ($k_{leak}[Ca^{2+}]_o$). One may ask why the platelet was not "designed" with a lower value of k_{leak}. We speculate that this is because the platelet would then have too low a resting $[Ca^{2+}]_{cyt}$ and that the dense tubules would not be able to accumulate the necessary amount of releasable Ca^{2+}. We have determined a K_m of 180 ± 5 nM and an n of 1.40 ± 0.05 for the dense tubular pump in "chemically skinned" platelets (Jy & Haynes, 1988).

The preliminary experiment shown in Fig. 14 gives evidence that Na^+-Ca^{2+} exchange is responsible for the linear portion of the $[Ca^{2+}]_{cyt}$ dependence of extrusion. This point will be addressed in greater detail in a future publication. The linear portion contributes only 19% of net efflux rate at 1.5 μM $[Ca^{2+}]_{cyt}$, but could perhaps make a contribution equal to the saturable component at $[Ca^{2+}]_{cyt} = 6$ μM. Rengasamy et al. (1987) have reported a Na^+-Ca^{2+} exchange activity in platelet membrane vesicles with a K_m of 20 μM. If this were identified with our nonsaturable component, the rate constant k_{linear} would then be equal to the V_m/K_m quotient of the exchanger. This would give a V_m value for efflux of approx. 1 μM/min, predicting that it would take the exchanger well over 10 min to reduce $[Ca^{2+}]_{cyt}$ from 10 to 1 μM. Experimental analysis directed at the activity of the exchanger and Ca^{2+} buffering capacity in this range may require the use of much lower-affinity indicators.

Conclusions

The present study has shown that Ca^{2+} buffering by quin2, thought to be a major drawback of the indicator, can actually be applied as a useful method for study of Ca^{2+} handling by the cell and of the Ca^{2+} pumps responsible for the same. The developed protocols allow for the quantitation of the cytoplasmic buffering capacity and the *in situ* characterization of the Ca^{2+} extrusion system located in the plasma membrane. Knowledge of the cytoplasmic Ca^{2+} binding characteristics will enable quantitative study of agonist-stimulated Ca^{2+} influx and release processes, expressing the results in nmol Ca^{2+} per liter cell volume, mg protein or other absolute measures. Such knowledge could provide a basis for mathematical modeling of platelet Ca^{2+} handling under a variety of conditions. We have used the quin2 overload procedure to show that elevation of cAMP and cGMP increase the rate of the extrusion process while phorbol ester is without effect (Johansson et al., 1988). The methods developed for studying active extrusion can also be applied to a number of other important problems, including the question of whether thrombin, collagen, ADP or arachidonic acid, etc., activate or suppress the extrusion system. The method can also be applied to the study of various platelet pathologies.

This work was supported by U.S. Public Health Services grant HL 07188 and Florida Heart Assn. We wish to thank the three journal referees for their critical readings of the manuscript and for comments, suggestions and criticisms which lead to its improvement. We also wish to thank Ms. Norma Jacobs for editorial assistance.

References

Ahn, Y.S., Jy, W., Harrington, W.J., Shanbaky, N., Fernandez, L.F., Haynes, D.H. 1987. Increased platelet calcium in thrombosis and related disorders and its correction by nifedipine. *Thromb. Res.* **45**:135–143

Baker, P.F. 1986. The sodium-calcium exchange system. *In:* Calcium and the Cell. D. Evered and J. Whelen, editors. pp. 73–92. Wiley, Chichester, UK

Bennett, J.P., Cockcroft, S., Gomperts, B.D. 1979. Ionomycin stimulates mast cell histamine secretion by forming a lipid-soluble calcium complex. *Nature (London)* **282**:851–853

Blaustein, M.P., Nelson, M.T. 1982. Sodium-calcium exchange: Its role in the regulation of cell calcium. *In:* Membrane Transport of Calcium. E. Carafoli, editor. pp. 217–236. Academic, New York

Brass, L.F. 1984*a*. Ca^{2+} homeostasis in unstimulated platelets. *J. Biol. Chem.* **259:**12563–12570

Brass, L.F. 1984*b*. The effect of Na^+ on Ca^{2+} homeostasis in unstimulated platelets. *J. Biol. Chem.* **259:**12571–12575

Brass, L.F. 1985. Ca^{2+} transport across the platelet plasma membrane. *J. Biol. Chem.* **260:**2231–2236

Carafoli, E. 1985. The homeostasis of calcium in heart cells. *J. Mol. Cell. Cardiol.* **17:**203–212

Carafoli, E., Zurini, M., Benaim, G. 1986. The calcium pump of plasma membranes. *In:* Calcium and the Cell. D. Evered and J. Whelen, editors. pp. 58–72. Wiley, Chichester, UK

Caroni, P., Carafoli, E. 1981. The Ca^{2+}-pumping ATPase of heart sarcolemma. Characterization, calmodulin dependence and partial purification. *J. Biol. Chem.* **256:**3263–3270

Chiu, V.C.K., Haynes, D.H. 1980. Rapid kinetic studies of active Ca^{2+} transport in sarcoplasmic reticulum. *J. Membrane Biol.* **56:**219–239

Cutler, L., Rodan, G., Feinstein, M.B. 1978. Cytochemical localization of adenylate cyclase and of calcium ion, magnesium ion-activated ATPases in the dense tubular system of human blood platelets. *Biochim. Biophys. Acta* **542:**357–371

DiPolo, R., Beauge, L. 1983. The calcium pump and sodium-calcium exchange in squid axons. *Annu. Rev. Physiol.* **45:**313–324

Enyedi, A., Sarkadi, B., Foldes-Papp, Z., Monostory, S., Gardos, G. 1986. Demonstration of two distinct calcium pumps in human platelet membrane vesicles. *J. Biol. Chem.* **261:**9558–9563

Feinstein, M.B. 1982. The role of calmodulin in hemostasis. *Prog. Hemost. Thromb.* **6:**25–61

Grynkiewicz, G., Poenie, M., Tsien, R.Y. 1985. A new generation of Ca^{2+} indicators with greatly improved fluorescence properties. *J. Biol. Chem.* **260:**3440–3450

Hack, N., Croset, M., Crawford, N. 1986. Studies on the bivalent-cation-activated ATPase activities of highly purified human platelet surface and intracellular membranes. *Biochem. J.* **233:**661–668

Hasselbach, W., Oetliker, H. 1983. Energetics and electrogenicity of the sarcoplasmic reticulum calcium pump. *Annu. Rev. Physiol.* **45:**325–339

Haynes, D.H., Mandveno, A. 1983. The pH dependence of the Ca^{2+}, Mg^{2+}-ATPase of sarcoplasmic reticulum: Evidence that the Ca^{2+} translocator bears a doubly negative charge. *J. Membrane Biol.* **74:**25–40

Haynes, D.H., Mandveno, A.R. 1987. Computer modeling of Ca^{2+} pump function of Ca^{2+}-Mg^{2+}-ATPase of sarcoplasmic reticulum. *Physiol. Rev.* **67:**244–284

Johansson, J.S., Nied, L.E., Haynes, D.H. 1988. Effects of activation of protein kinases A, C, and G on the kinetics of the Ca^{2+} extrusion system of the human platelet. *FASEB J.* **2:**A398

Jy, W., Ahn, Y.S., Shanbaky, N., Fernandez, L.F., Harrington, W.J., Haynes, D.H. 1987. Abnormal calcium handling by platelets in thrombotic disorders. *Circ. Res.* **60:**346–355

Jy, W., Haynes, D.H. 1984. Intracellular calcium storage and release in the human platelet: Chlortetracycline as a continuous monitor. *Circ. Res.* **55:**595–608

Jy, W., Haynes, D.H. 1987. Thrombin-induced calcium movements in platelet activation. *Biochim. Biophys. Acta* **929:**88–102

Jy, W., Haynes, D.H. 1988. Calcium uptake and release characteristics of the dense tubules of digitonin-permeabilized human platelets. *Biochim. Biophys. Acta* (*in press*)

Kohse, K.P., Heilmeyer, L.M.G., Jr. 1981. The effect of Mg^{2+} on the Ca^{2+}-binding properties and Ca^{2+}-induced tyrosine-fluorescence changes of calmodulin isolated from rabbit skeletal muscle. *Eur. J. Biochem.* **117:**507–513

Liu, C., Hermann, E.T. 1978. Characterization of ionomycin as a calcium ionophore. *J. Biol. Chem.* **253:**5892–5894

MacIntyre, D.E., Bushfield, M., Shaw, A.M. 1985. Regulation of platelet cytosolic free calcium by cyclic nucleotides and protein kinase C. *FEBS Lett.* **188:**383–388

Melzer, W., Rios, E., Schnider, M.F. 1986. The removal of myoplasmic free calcium following calcium release in frog skeletal muscle. *J. Physiol. (London)* **372:**261–292

Menashi, S., Davis, C., Crawford, N. 1982. Calcium uptake associated with an intracellular membrane fraction prepared from human blood platelets by high-voltage, free-flow electrophoresis. *FEBS Lett.* **140:**298–302

Mustard, J.F., Perry, D.W., Ardlie, N.G., Packham, M.A. 1972. Preparation of suspensions of washed platelets from humans. *Br. J. Haematol.* **22:**193–204

Niggli, V., Penniston, J.T., Carafoli, E. 1979. Purification of the (Ca^{2+}-Mg^{2+})-ATPase from human erythrocyte membranes using a calmodulin affinity column. *J. Biol. Chem.* **254:**9955–9958

Pollock, W.K., Rink, T.J. 1986. Thrombin and ionomycin can raise platelet cytosolic Ca^{2+} to micromolar levels by discharge of internal stores: Studies using fura-2. *Biochem. Biophys. Res. Commun.* **139:**308–314

Pollock, W.K., Rink, T.J., Irvine, R.F. 1986. Liberation of [^{3}H]arachidonic acid and changes in cytosolic free calcium in fura-2-loaded human platelets stimulated by ionomycin and collagen. *Biochem. J.* **235:**869–877

Pressman, B.C. 1973. Properties of ionophores with broad range of specificity. *Fed. Proc.* **32:**1698–1703

Rao, G.H.R., Peller, J.D., Semba, C.P., White, J.G. 1986. Influence of the calcium-sensitive fluorophore, quin2, on platelet function. *Blood* **67:**354–361

Rao, G.H.R., Peller, J.D., White, J.G. 1985. Measurement of ionized calcium in blood platelets with a new generation calcium indicator. *Biochem. Biophys. Res. Commun.* **132:**652–657

Rengasamy, A., Soura, S., Feinberg, H. 1987. Evidence for Na^+-Ca^{2+} exchange activity in platelet plasma membranes. *Fed. Proc.* **46:**721

Rink, T.J., Sanchez, A. 1984. Effects of prostaglandin I_2 and forskolin on the secretion from platelets evoked at basal concentrations of cytoplasmic free calcium by thrombin, collagen, phorbol ester and exogenous diacylglycerol. *Biochem. J.* **222:**833–836

Rink, T.J., Smith, S.W., Tsien, R.Y. 1982. Cytoplasmic free Ca^{2+} in human platelets: Ca^{2+} thresholds and Ca-independent activation for shape-change and secretion. *FEBS Lett.* **148:**21–26

Sage, S.O., Rink, T.J. 1985. Inhibition by forskolin of cytosolic calcium rise, shape change and aggregation in quin2-loaded human platelets. *FEBS Lett.* **188:**135–140

Schatzmann, H.J. 1982. The plasma membrane Ca^{2+} pump of erythrocytes and other animal cells. *In:* Membrane Transport of Calcium. E. Carafoli, editor. pp. 41–108. Academic, New York

Shanbaky, N.M., Ahn, Y.S., Jy, W., Harrington, W.J., Fernandez, L.F., Haynes, D.H. 1987. Abnormal aggregation accompanies abnormal platelet Ca^{2+} handling in arterial thrombosis. *Thromb. Haemostas.* **57:**1–10

Sixma, J.J., Lips, J.P.M. 1978. Isolation of platelet membranes: A review. *Thrombos. Haemostas.* **39:**328–337

Stahl, K., Themann, H., Dame, W.R. 1978. Ultrastructural mor-

phometric investigations on normal human platelets. *Haemostasis* **7**:242–251

Steiner, B., Luscher, E.F. 1985. Evidence that the platelet plasma membrane does not contain a (Ca^{2+} + Mg^{2+})-dependent ATPase. *Biochim. Biophys. Acta* **818**:299–309

Thompson, N.T., Scrutton, M.C. 1985. Intracellular calcium fluxes in human platelets. *Eur. J. Biochem.* **147**:421–427

Trevorrow, K., Haynes, D.H. 1984. The thermodynamic efficiency of the Ca^{2+}-Mg^{2+}-ATPase is one hundred percent. *J. Bioenerg. Biomembr.* **16**:53–59

Tscharner, V. von, Deranleau, D.A., Baggiolini, M. 1986. Calcium fluxes and calcium buffering in human neutrophils. *J. Biol. Chem.* **261**:10163–10168

Tsien, R.Y., Pozzan, T., Rink, T.J. 1982. Calcium homeostasis in intact lymphocytes: Cytoplasmic free calcium monitored with a new, intracellularly trapped fluorescent indicator. *J. Cell Biol.* **94**:325–334

Verjovski-Almeida, S., Inesi, G. 1979. Fast-kinetic evidence for an activating effect of ATP on the Ca^{2+} transport of sarcoplasmic reticulum ATPase. *J. Biol. Chem.* **254**:18–21

White, G.C., Levine, S.N., Steiner, A.N. 1981. Platelet calcium-dependent proteins: Identification and localization of the calcium-dependent regulator, calmodulin, in platelets. *Am. J. Hematol.* **101**:359–367

Received 14 January 1988; revised 18 May 1988

Appendix

Implicit to our treatment is the fact that the free internal ("ionized") calcium (Ca^{2+}_{cyt}) is an insignificant fraction of the total intracytoplasmic calcium (Ca^{2+}_{i}). There are two pools of Ca^{2+}_{i} in quin2-loaded platelets: (i) the Ca^{2+} bound to quin2 (Ca-Q), and (ii) the Ca^{2+} bound to intrinsic cytoplasmic binding sites (Ca-*B*). Both pools are in equilibrium with $[Ca^{2+}]_{cyt}$ which is reported by quin2. The complexation properties of quin2 are known and can be used to determine both $[Ca^{2+}]_{cyt}$ and [Ca-Q]. The equilibrium, expressed as a dissociation, is given by

$$K_Q = ([Ca^{2+}]_{cyt} \cdot [Q])/[Ca\text{-}Q] \quad (A1)$$

where K_Q is the K_d of the Ca-Q complex. Using the conservation equation for total quin2 it can be shown that

$$[Ca\text{-}Q] = ([Q]_T \cdot [Ca^{2+}]_{cyt})/(K_Q + [Ca^{2+}]_{cyt}). \quad (A2)$$

where $[Q]_T$ is the total concentration of dye in the cytoplasm. Thus a known quin2 concentration will make a known contribution to the total Ca^{2+} binding capacity of the cytoplasm.

Drawing on our undergraduate training in chemistry and mathematics, we find it useful to consider these processes in differential form. A useful quantity is the change in [Ca-Q] which results in a small change in $[Ca^{2+}]_{cyt}$. This is given by $d[Ca\text{-}Q]/d[Ca^{2+}]_{cyt}$ which, for lack of a suitable precedent in the biological literature, we will define as the Differential Binding Capacity. It is given by

$$d[Ca\text{-}Q]/d[Ca^{2+}]_{cyt} = ([Q]_T \cdot K_Q)/(K_Q + [Ca^{2+}]_{cyt})^2. \quad (A3)$$

which is obtained by differentiating Eq. (A2) with respect to $[Ca^{2+}]_{cyt}$. All quantities of Eq. (A3) are known in a particular experiment.

The intrinsic cytoplasmic Ca^{2+} binding proteins also make a contribution to the differential binding capacity of the cytoplasm ($d[Ca\text{-}B]/d[Ca^{2+}]_{cyt}$). This contribution, which is also a function of $[Ca^{2+}]_{cyt}$, is initially unknown, but can be determined as shown below. The total differential binding capacity of the cytoplasm ($d[Ca\text{-}T]/d[Ca^{2-}]_{cyt}$) is

$$d[Ca\text{-}T]/d[Ca^{2+}]_{cyt} = (d[Ca\text{-}Q]/d[Ca^{2+}]_{cyt}) + (d[Ca\text{-}B]/d[Ca^{2+}]_{cyt}) \quad (A4)$$

where [Ca-*T*] = [Ca-Q] + [Ca-*B*]. Melzer, Rios and Schnider (1986) have applied a similar concept (which they called "intrinsic expansion") to the analysis of Antipyrylazo III data in frog skeletal muscle.

Substituting Eq. (A3) into Eq. (A4) gives

$$d[Ca\text{-}T]/d[Ca^{2+}]_{cyt} = \frac{[Q]_T \cdot K_Q}{(K_Q + [Ca^{2+}]_{cyt})^2} + (d[Ca\text{-}B]/d[Ca^{2+}]_{cyt}) \quad (A5)$$

When a pump removes a Ca^{2+} from the cytoplasm, the Ca^{2+} may have come from either Ca-Q or Ca-*B*. According to the above formalism, the probability that a given Ca^{2+} will come off Ca-Q, and therefore result in a fluorescence change, can be expressed as

$$P = \frac{d[Ca\text{-}Q]/d[Ca^{2+}]_{cyt}}{(d[Ca\text{-}Q]/d[Ca^{2+}]_{cyt}) + (d[Ca\text{-}B]/d[Ca^{2+}]_{cyt})} \quad (A6)$$

or

$$P = \frac{\frac{[Q]_T \cdot K_Q}{(K_Q + [Ca^{2+}]_{cyt})^2}}{\frac{[Q]_T \cdot K_Q}{(K_Q + [Ca^{2+}]_{cyt})^2} + \frac{d[Ca\text{-}B]}{d[Ca^{2+}]_{cyt}}}. \quad (A7)$$

This equation predicts that P will have to be "hyperbolic" or "saturation" function of $[Q]_T$ for any particular $[Ca^{2+}]_{cyt}$. Thus for small $[Q]_T$, P will be proportional to $[Q]_T$ and will approach the limit of 1.0 for large $[Q]_T$. The equation bears intuitive similarity to the Michaelis-Menten equation. It is possible to define a $[Q]_{T,1/2}$ at which $P = 0.5$ for the condition

$$[Q]_{T,1/2} \cdot \frac{K_Q}{(K_Q + [Ca^{2+}]_{cyt})^2} = \frac{d[Ca\text{-}B]}{d[Ca^{2+}]_{cyt}}. \quad (A8)$$

This condition was determined experimentally and used to define the binding characteristics of the cytoplasmic proteins (*cf.* Figs. 10 and 11).

The value of P can be determined directly from the dependence of the observed rate of removal of Ca^{2+} from Ca-Q by the pump ($Rate_{obs}$) with the pump operating at defined $[Ca^{2+}]_{cyt}$ but

with variable $[Q]_T$. Thus

$$\text{Rate}_{obs} = d[\text{Ca-Q}]/dt. \tag{A9}$$

From Eqs. (A6), (A7) and (A9) we obtain

$$\text{Rate}_{obs} = \text{Rate}_{max} \cdot P \tag{A10}$$

where Rate_{max} is the true rate of the extrusion mechanism measurable at $P = 1.0$.

A convenient method of determination of $[Q]_{T,1/2}$ and validation of the method is to plot $1/\text{Rate}_{obs}$ *vs.* $1/[Q]_T$ at fixed $[Ca^{2+}]_{cyt}$. A linear relationship such as presented in Fig. 9 should be obtained. Combining Eqs. (A7) and (A10) and casting the result in reciprocal fashion gives

$$(1/\text{Rate}_{obs}) = 1/\text{Rate}_{max}\left(1 + \frac{d[\text{Ca-}B]/d[Ca^{2+}]_{cyt}}{[Q]_T \cdot \dfrac{K_Q}{(K_Q + [Ca^{2+}]_{cyt})^2}}\right) \tag{A11}$$

which, of course, yields a double reciprocal plot and allows for facile determination of Rate_{max} and $d[\text{Ca-}B]/d[Ca^{2+}]_{cyt}$ as defined in Eq. (A8).

Experimentally, double reciprocal plots of Rate_{obs} and $[Q]_T$ are constructed for every $[Ca^{2+}]_{cyt}$ for which accurate rate data is available. The result is a family of straight lines, each defining the Rate_{max} and $[Q]_{T,1/2}$ values for the applicable $[Ca^{2+}]_{cyt}$. The Rate_{max} data define the $[Ca^{2+}]_{cyt}$ dependence of the extrusion system. As will be shown below, the $[Q]_{T,1/2}$ values can be used to derive the binding characteristics of the cytoplasmic proteins.

Insertion of the $[Q]_{T,1/2}$ values, their corresponding $[Ca^{2+}]_{cyt}$ values and K_q (= 115 nM) into the left-hand portion of Eq. (A8) yields $d[\text{Ca-}B]/d[Ca^{2+}]_{cyt}$ as a function of $[Ca^{2+}]_{cyt}$. This is shown in Fig. 10. In the general case, this curve would be numerically integrated to yield $[\text{Ca-}B]$ *vs.* $[Ca^{2+}]_{cyt}$. In our specific case the $d[\text{Ca-}B]/d[Ca^{2+}]_{cyt}$ *vs.* $[Ca^{2+}]_{cyt}$ conforms to the Ca-*B* analogue of Eq. (A3) in which "*B*" is substituted for "Q" (with different numerical values, of course). This is sufficient to characterize the cytoplasmic binding elements contributing between 50 nM $< [Ca^{2+}]_{cyt} <$ 1,500 nM as a single class of noninteracting sites.